

# Relationships between Antiviral Treatment Effects and Biphasic Viral Decay Rates in Modeling HIV Dynamics

A. Adam Ding and Hulin Wu

## ABSTRACT

Recently potent combination antiviral therapies, which consist of reverse transcriptase inhibitor (RTI) drugs and protease inhibitor (PI) drugs, can rapidly suppress HIV below the limit of detection. Two phases of plasma viral decay after initiation of treatment were observed from clinical studies. Some researchers have suggested that the viral decay rates may reflect the potency (efficacy) of antiviral therapies. In this paper we model the effect of RTI drugs and PI drugs as inhibition rates of cell infection and infectious virus production, respectively, based on the biological mechanisms of these two different types of drugs. Through rigorous mathematical derivation, we show that the two viral decay rates are monotone functions of the treatment effects of these antiviral therapies. Approximation formulas for the relationships between viral decay rates and treatment effects are constructed. Computer simulations show that the approximation formulas approximate the true values very well. These formulas may be used to study what factors really affect the viral decay rates. The results in this paper provide a theoretical justification for using both viral decay rates for evaluation of treatment efficacy of antiviral therapies.

**Key words:** AIDS, antiviral therapy, differential equations, HIV infection, viral dynamics.

## 1. INTRODUCTION

Modeling the interaction of the human immunodeficiency virus (HIV) with its host cells can be traced back to a decade ago [1, 2, 3, 4]. Most of these earlier models were developed to explain biological phenomena observed from clinical studies, via computer simulations. In the last four years, simplified version of these HIV dynamic models were directly applied to clinical data and important biological parameters of HIV and its host cells were obtained [5, 6, 7, 8]. This led to a new understanding of the pathogenesis of HIV infection. Recently highly active antiretroviral therapies (HAART), which consist of reverse transcriptase inhibitor (RTI) drugs and potent protease inhibitor (PI) drugs, can rapidly suppress HIV in plasma below detectable levels. Two phases of plasma viral decay rates were observed from clinical studies [8, 9, 10]. Some researchers suggested that the viral decay rates may reflect the potency (efficacy) of antiviral therapies [11, 12, 13]. Although Essunger et al. [11] showed that the first viral decay rate is directly related to treatment efficacy, relationships between biphasic viral decay rates and treatment efficacies in two infected cell compartments have not been studied in detail.

In this paper we intend to study the effect of potency (efficacy) of antiviral therapies on biphasic viral decays by modeling viral dynamics. In Section 2, we describe a basic viral dynamic model and a model with antiviral treatment. We study the relationships between viral decay rates and treatment effects in Section 3. Section 4 gives some discussions on evaluation of treatment efficacy using viral decay rates. We summarize our conclusions and provide further discussions in Section 5. Some technical proofs are deferred to the appendices.

## 2. VIRAL DYNAMIC MODELS

Perelson et al. [8] have modeled two phases of plasma viral decay assuming that there are two major HIV-infected cell compartments: productively infected cells and long-lived

infected cells. Other virus compartments such as latently infected cells may also exist, but these compartments cannot be identified from plasma viral load measurements [8] and we will not consider them in our model. The following variables are considered in our model: (1) uninfected target cells, such as T cells and macrophages; (2) productively infected cells, infected cells which are actively producing virus; (3) long-lived infected cells, such as macrophages, that are chronically infected and long-lived; (4) infectious virus, virus that are functional and capable of infecting target cells; (5) noninfectious virus, virus that are dysfunctional and cannot infect target cells. We denote the concentration of these cells and virus by  $T, T_1, T_2, V_I$ , and  $V_{NI}$ , respectively. The basic viral dynamic model which is modified from Perelson et al. [7, 8] is described as follows.

Infectious HIV virions ( $V_I$ ) may infect target cells ( $T$ ) and turn them into infected cells at a rate of  $kTV_I$ . Among these infected cells, we assume  $\alpha_1$  to be the proportion of productively infected cells ( $T_1$ ) and  $\alpha_2$  to be the proportion of long-lived infected cells ( $T_2$ ). The infected cells,  $T_1$  and  $T_2$ , may die at rates  $\delta_1$  and  $\delta_2$  after producing an average of  $N_1$  and  $N_2$  virions per cell during their lifetimes, respectively. Due to replication errors, the majority of virions produced from infected cells are dysfunctional (noninfectious) and can not infect target cells [14]. We denote  $\eta_0$  as the proportion of noninfectious virus in the total virus pool before the intervention of antiviral drugs, and denote  $c$  as the clearance rates of free virions. The basic viral dynamic model before treatment can be written as follows:

$$\begin{aligned}
\frac{d}{dt}T_1 &= \alpha_1 kTV_I - \delta_1 T_1 \\
\frac{d}{dt}T_2 &= \alpha_2 kTV_I - \delta_2 T_2 \\
\frac{d}{dt}V_I &= (1 - \eta_0)(N_1\delta_1 T_1 + N_2\delta_2 T_2) - cV_I \\
\frac{d}{dt}V_{NI} &= \eta_0(N_1\delta_1 T_1 + N_2\delta_2 T_2) - cV_{NI}.
\end{aligned} \tag{1}$$

Notice that we may separate the target cells  $T$  into T cells and long-lived cells (such as macrophages) as Perelson et al. [8] did. This separation will produce equivalent mathematical results, but the biological difference should be noted. The second infected cell

compartment ( $T_2$ ) may also be considered as the latently infected cells and may be modeled as in Perelson et al. [8]. But these alternatives will lead to similar mathematical results. Some experimental evidence shows that infected cells may produce virus continuously during their lifetime. In this case, the viral production rate,  $N_1\delta_1T_1$  or  $N_2\delta_2T_2$ , may be replaced by a constant. However, this replacement will not change our mathematical results.

**Place of Figure 1**

The process of HIV replication and the intervention of antiviral drugs are shown in Figure 1. RTI drugs (including non-nucleoside RTI drugs and nucleoside analogues) are designed to prevent the conversion of HIV RNA to DNA in the early stage of HIV replication. Thus RTI drugs block the conversion (infection) of uninfected cells to actual infected cells (cells that can produce virus). We assume that RTI drugs reduce the infection rates in the two infected cell compartments,  $T_1$  and  $T_2$ , by factors  $(1 - \gamma_1)$  and  $(1 - \gamma_2)$ , respectively. PI drugs are designed to intervene in the last stage of the virus replication cycle to prevent HIV from being properly assembled, and thus cause the newly produced virus to be noninfectious. Hence the effect of PI drugs is to reduce the proportion of infectious virus ( $V_I$ ) in the newly produced virus. We assume that PI drugs reduce the proportions of infectious virus produced from productively infected cells ( $T_1$ ) and long-lived infected cells ( $T_2$ ) by factors  $(1 - \eta_1)$  and  $(1 - \eta_2)$ , respectively. Thus, the viral dynamic model after

initiation of antiviral therapy which consists of both RTI and PI drugs can be written as

$$\begin{aligned}
\frac{d}{dt}T_1 &= (1 - \gamma_1)\alpha_1kTV_I - \delta_1T_1 \\
\frac{d}{dt}T_2 &= (1 - \gamma_2)\alpha_2kTV_I - \delta_2T_2 \\
\frac{d}{dt}V_I &= (1 - \eta_0)[(1 - \eta_2)N_2\delta_2T_2 + (1 - \eta_1)N_1\delta_1T_1] - cV_I \\
\frac{d}{dt}V_{NI} &= (\eta_0 + (1 - \eta_0)\eta_2)N_2\delta_2T_2 + (\eta_0 + (1 - \eta_0)\eta_1)N_1\delta_1T_1 - cV_{NI}.
\end{aligned} \tag{2}$$

The overall treatment effects in the two infected cell compartments,  $T_1$  and  $T_2$ , can then be defined as  $e_1 = 1 - (1 - \gamma_1)(1 - \eta_1)$  and  $e_2 = 1 - (1 - \gamma_2)(1 - \eta_2)$ , respectively. If  $e_1 = 0$ , the treatment has no effect for blocking virus replication from productively infected cells; if  $e_1 = 1$ , the treatment completely blocks virus replication from productively infected cells. Similarly  $e_2 = 0$  means no effect and  $e_2 = 1$  means complete inhibition of virus replication from the second compartment, long-lived infected cells. Also notice that  $e_i$  is a monotone increasing function of  $\eta_i$  and  $\gamma_i$  ( $i = 1, 2$ ). As mentioned above, RTI and PI drugs intervene the viral replication at different stages. Factor,  $(1 - \gamma_i)$  can be interpreted as the with/without RTI-drug treatment ratio of cell infection and  $(1 - \eta_i)$  as the with/without PI-drug treatment ratio of viral production from each infected cell. Using the multiplication rule, factor  $(1 - \gamma_1)(1 - \eta_1)$  will be the with/without RTI-PI-combination treatment ratio of total viral production in the whole viral replication cycle. Thus,  $e_1 = 1 - (1 - \gamma_1)(1 - \eta_1)$  and  $e_2 = 1 - (1 - \gamma_2)(1 - \eta_2)$  will be the overall inhibition rates of viral production due to RTI-PI-combination treatments in two different infected cell compartments. If a treatment is potent in the first compartment (productively infected cells), one may conceive that it is also potent in the second compartment (long-lived/latently infected cells). This means that  $\gamma_1$ ,  $\eta_1$ , and  $e_1$  may be positively correlated with  $\gamma_2$ ,  $\eta_2$ , and  $e_2$  in general. However, we cannot eliminate the possibility that some drugs may work well in the first compartment, but not in the second compartment, and vice versa.

If we assume the concentration of target cells ( $T$ ) to be constant as in Perelson et al.

[7, 8], we can solve the above system of differential equations and obtain the following closed-form solution for total virus (see Appendix A):

$$V(t) = V_I(t) + V_{NI}(t) = P_0e^{-d_0t} + P_0e^{-ct} + P_1e^{-d_1t} + P_2e^{-d_2t}. \quad (3)$$

In fact, the assumption of constant  $T$  is reasonable in many situations, and simulation studies show that the slight recovery of target T cells during treatment has little effect on our results [15].

As noticed by Perelson et al. [7] and Herz et al. [16], there exists a small ‘shoulder’ in plasma virus during the first few days of potent antiviral treatment. This small ‘shoulder’ may be caused by two reasons: (i) pharmacological and intracellular delay; and (ii) the virus released from previous infection cycles which is indicated by terms  $P_0e^{-d_0t} + P_0e^{-ct}$  in equation (3). The small ‘shoulder’ will disappear after 2 or 3 days of treatment [7, 15, 16]. Then the viral load follows a rapid exponential decay which is dominated by the term  $P_1e^{-d_1t}$ . The decay becomes slower after several weeks which is mainly due to the term  $P_2e^{-d_2t}$  in the model (3). In practice, viral load may not be measured frequently during the ‘shoulder’ in most AIDS clinical trials. The viral load data after the ‘shoulder’ can be nicely approximated by a bi-exponential model [15]

$$V(t) = P_1e^{-d_1t} + P_2e^{-d_2t}, \quad t \geq t_c, \quad (4)$$

where  $t_c$  is the time that the ‘shoulder’ disappears (usually 2 or 3 days). This bi-exponential model describes the observed biphasic decay of plasma virus very well [8, 15]. Also, in the next section we show (Figure 2) that this bi-exponential model approximates the complete model (3) almost perfectly in our simulation studies.

### 3. RELATIONSHIPS BETWEEN VIRAL DECAY RATES AND TREATMENT EFFECTS

#### 3.1 VIRAL DECAY RATES AS MONOTONE FUNCTIONS OF TREATMENT EFFECTS

The parameters in the bi-exponential model (4) are complicated nonlinear functions of the biological parameters in (2) (see Appendix A). To yield simpler biological interpretation of the parameters,  $d_1, d_2, P_1$  and  $P_2$  in (4), the treatment effects were often considered as perfect, i.e.,  $e_1 = e_2 = 1$ , and the pretreatment steady-state assumption was made [7, 8]. In this case,  $d_1 = \delta_1$  and  $d_2 = \delta_2$  are respectively the clearance rates of the first compartment  $T_1$  (productively infected cells) and the second compartment  $T_2$  (long-lived infected cells), and  $P_1$  and  $P_2$  can also be represented by simple functions of biological parameters in (2) [7, 8, 15].

However, the perfect treatment assumption is not realistic in practice. It is impossible to completely shut down viral replication after initiation of antiviral therapy. In this situation, the two decay rates,  $d_1$  and  $d_2$ , are no longer exactly  $\delta_1$  and  $\delta_2$ , the clearance rates of  $T_1$  and  $T_2$ . The following theorem gives the key relationships between the viral decay rates and the treatment effects.

**Theorem 1** *In the solution (3), assuming  $\delta_2 < \delta_1 < c$ , we have the following results:*

(a) *For all  $0 \leq e_1, e_2 < 1$ , the three apparent viral decay rates satisfy the following relationship*

$$d_2 < \delta_2 < d_1 < \delta_1 < c < d_0$$

(b) *For any fixed  $e_2$ ,  $d_1$  and  $d_2$  are monotone increasing functions of  $e_1$  while  $d_0$  is a monotone decreasing function of  $e_1$ . For any fixed  $e_1$ ,  $d_2$  is a monotone increasing function of  $e_2$  while  $d_0$  and  $d_1$  are monotone decreasing function of  $e_2$ .*

Proof: see Appendix B.

### 3.2 APPROXIMATION FORMULAS

Theorem 1 establishes the monotone relationships between the viral decay rates and the treatment efficacies. However, simple analytic relationships are needed to study how viral decay rates relate to treatment effects and other factors. Based on the fact,  $c \gg d_1 \gg d_2$ , observed from clinical studies [7, 8, 17], we can approximate  $d_1$  and  $d_2$  by ignoring small terms with order  $O(\frac{\delta_1}{c})$  and  $O(\frac{\delta_2}{\delta_1})$ . To obtain our approximation formulas for  $d_1$  and  $d_2$ , first we need to establish that the  $d_0$  and  $d_1$  are of the same order as  $c$  and  $\delta_1$  respectively. We sketch the derivation of the approximation formulas as follows (some technical parts are included in Appendices).

(i)  $d_0 \approx c$ .

Denote  $r_1 = (1 - \eta_0)N_1\alpha_1kT$  and  $r_2 = (1 - \eta_0)N_2\alpha_2kT$  as viral production rates from the two infected cell compartments,  $T_1$  and  $T_2$ , respectively (Appendix A). If we assume that the system is in a quasi-steady state before treatment, then we have  $r_1 + r_2 = c$ , i.e., total viral production equals total viral clearance. Notations  $d_0(e_1, e_2)$ ,  $d_1(e_1, e_2)$  and  $d_2(e_1, e_2)$  are used to indicate that the parameters  $d_0$ ,  $d_1$  and  $d_2$  are functions of treatment efficacies,  $e_1$  and  $e_2$ . If  $e_1 = e_2 = 0$ , we can easily show that  $d_2(0, 0) = 0$  and  $d_0(0, 0) < c + \delta_1$  by directly calculating the eigenvalues of matrix  $\bar{A}$  in Appendix A. Theorem 1 then implies that  $0 = d_2(0, 0) \leq d_2 < \delta_2 < d_1 < \delta_1 < c < d_0 \leq d_0(0, 0) < c + \delta_1$ . The result,  $c \leq d_0 < c + \delta_1$  indicates that  $d_0 \approx c$  by ignoring the small term of order  $O(\frac{\delta_1}{c})$ .

(ii)  $d_1$  is of the same order as  $\delta_1$ .

Since  $d_2 < \delta_2$ , we have  $\frac{d_1(e_1, e_2) - \delta_2}{d_1(e_1, e_2) - d_2(e_1, e_2)} \leq 1$ . Using this fact and the results from (10) and (14) in Appendix B, the  $d_1$  is bounded from below by

$$\delta_1 + \delta_1 r_1 \int_{x=e_1}^1 \frac{1}{-c} dx = \delta_1 - \delta_1 \frac{r_1}{c} (1 - e_1). \quad (5)$$

Also from the quasi-steady state condition,  $r_1 + r_2 = c$ , we have  $r_1 < c$ . Hence we obtain

$d_1 > \delta_1 - \delta_1(1 - e_1) = e_1\delta_1$ . Since  $e_1\delta_1 < d_1 < \delta_1$ , the  $d_1$  is of the same order as  $\delta_1$  if  $e_1$  is not too small.

(iii) Approximation of  $d_1$  and  $d_2$ .

From the result of above (ii) and  $\delta_2 > d_2$  (Theorem 1), we have  $\frac{d_1 - \delta_2}{d_1 - d_2} = 1 + O(\frac{\delta_2}{\delta_1})$ . Then we can see that the differences between  $d_1$  and its lower bound (5) are small terms of order  $O(\frac{\delta_2}{\delta_1})$  and  $O(\frac{\delta_1}{c})$ . If we ignore these small terms, we obtain,

$$d_1 = \delta_1 - \delta_1 \frac{r_1}{c} (1 - e_1).$$

Similarly, from equation (21) in Appendix C and by ignoring the small terms of order  $O(\frac{\delta_2}{\delta_1})$  and  $O(\frac{\delta_1}{c})$ , we can obtain,

$$\begin{aligned} d_2 &= \delta_2 + \delta_2 r_2 \int_{x=e_2}^1 \frac{1}{-c} \frac{\delta_1}{\delta_1 - \delta_1 \frac{r_1}{c} (1 - e_1)} dx \\ &= \delta_2 - \delta_2 \frac{r_2}{c} \frac{1 - e_2}{1 - \frac{r_1}{c} (1 - e_1)}. \end{aligned}$$

(iv) Further simplification.

Clinical studies [8, 17] show that productively infected cells ( $T_1$ ) dominate long-lived infected cells ( $T_2$ ) in producing virus. The production ratio of  $T_2$  versus  $T_1$ ,  $r_2/r_1$ , was estimated to be less than 10% [8, 17]. Hence by ignoring a term of order  $(r_2/c)^2 < 1\%$ , the above formula for  $d_2$  can be further simplified to

$$d_2 = \delta_2 - \delta_2 \frac{r_2}{c} \frac{1 - e_2}{e_1}.$$

If we can ignore the small terms of order  $r_2/c < 10\%$ , the approximation formula of  $d_1$  can be further simplified to

$$d_1 = e_1\delta_1. \tag{6}$$

This is the result obtained by Essunger, et al. [11].

In summary, we have

$$d_1 = \left[1 - \frac{r_1}{c}(1 - e_1)\right]\delta_1, \quad (7)$$

$$d_2 = \left(1 - \frac{r_2}{c} \frac{1 - e_2}{e_1}\right)\delta_2, \quad (8)$$

where  $r_1 = (1 - \eta_0)N_1\alpha_1kT$  and  $r_2 = (1 - \eta_0)N_2\alpha_2kT$  are the viral production rates from compartments  $T_1$  and  $T_2$  before antiviral treatment. From these results, we can see that the two viral decay rates are functions of the treatment effects,  $e_1$  and  $e_2$ ; the clearance rates of the two compartments,  $\delta_1$  and  $\delta_2$ ; and the initial viral production/clearance ratio of the two compartments,  $r_1/c$  and  $r_2/c$ .

### 3.3 SIMULATION STUDIES ON THE APPROXIMATION MODEL AND FORMULAS

Approximation formulas (7) and (8) are obtained by ignoring small terms in calculating the eigenvalues of the coefficient matrix of the viral dynamic model. The approximation model (4) is obtained by ignoring the earlier shoulder of the viral load trajectory after treatment. To evaluate these approximation formulas, we conducted simulation studies using the parameters listed in Table 1. These parameter values were obtained from published literature or estimated from clinical data. When we varied the parameters in Table 1 in some reasonable ranges, the simulation results were quite similar.

<b>Place of Table 1</b>
-------------------------

First we numerically solved the differential equations (2) with the parameters in Table 1 and obtained total viral load  $V(t) = V_I(t) + V_{NI}(t)$ ,  $t = t_1, t_2, \dots, t_n$ . To see how good the approximation of bi-exponential model (4) is, we fitted the data of  $V(t)$  from numerical solutions of (2) for  $t \geq 2$  days to the bi-exponential model using the nonlinear

least squares method [15]. We plot the results for two simulation cases in Figure 2. The first is a potent treatment case ( $\gamma_1 = 0.5, \gamma_2 = 0.3, \eta_1 = 0.8, \eta_2 = 0.6, e_1 = 0.9, e_2 = 0.72$ ); another case is a weak treatment ( $\gamma_1 = \gamma_2 = \eta_1 = \eta_2 = 0.1, e_1 = e_2 = 0.19$ ). The cross (+) in Figure 2 is the simulated result from Model (4). We can see that the approximation of model (4), even with estimation error, is almost perfect in both simulation cases.

**Place of Figure 2**

To evaluate the approximation formulas (7) and (8), we first calculated  $d_1$  and  $d_2$  using formulas (7) and (8) with the true parameter values in above two cases. For the stronger treatment case ( $e_1 = 0.9, e_2 = 0.72$ ), the approximation error is extremely small (1.5% for  $d_1$  and 0.0% for  $d_2$ ). Even for the weak treatment case ( $e_1 = e_2 = 0.19$ ), the approximation error is still reasonable (2.3% for  $d_1$  and 11.1% for  $d_2$ ). We also plugged these approximate values of  $d_1$  and  $d_2$  in the bi-exponential model (4) to estimate total viral load  $V(t)$  (parameters  $P_1$  and  $P_2$  were taken to be the same as estimated above). The estimated  $V(t)$  is also plotted in Figure 2 (indicated by  $\circ$ ). The approximation is fairly decent. To investigate the behavior of the approximation formulas (7) and (8) for different combinations of  $e_1$  and  $e_2$ , we obtained the true values of  $d_1$  and  $d_2$  by calculating the eigenvalues of matrix  $\bar{A}$  in Appendix A numerically and the approximate values of  $d_1$  and  $d_2$  from formulas (7) and (8) for a large range of  $e_1$  and  $e_2$  combinations. For comparisons, the true values of  $d_1$  and  $d_2$  and the estimates of  $d_1$  and  $d_2$  from our approximation formulas are plotted in Figure 3. We can see that the approximation of  $d_1$  is pretty good within our simulation ranges of  $e_1$  and  $e_2$  (the error is less than 10%). The approximation of  $d_2$  is also reasonable except for some very weak treatment cases (small  $e_1$  cases). We also notice that, the stronger the treatment is, the better the approximation.

This is not surprising, since our approximation formulas are obtained by ignoring the small terms when the treatment is strong.

**Place of Figure 3**

#### 4. EVALUATION OF TREATMENT EFFICACY USING VIRAL DECAY RATES

The results in Section 3 provide a theoretical justification for using both viral decay rates to evaluate efficacy of antiviral therapies. If a treatment (say A) is more potent in blocking virus replication compared to Treatment B, Theorem 1 shows that both phases of viral decays should be faster in patients with Treatment A. Thus, antiviral potency of treatments can be assessed by comparing their viral decay rates.

The approximation formulas (7) and (8) in Section 3.2 provide analytic relationships between treatment effects and viral decay rates. These results illustrate more clearly how the change in treatment efficacies lead to changes in the viral decay rates. As we argued previously [8, 17],  $\frac{r_1}{c} \geq 0.9$  and  $\frac{r_2}{c} \leq 0.1$ . We take  $\frac{r_1}{c} = 0.9$ ,  $\frac{r_2}{c} = 0.1$ ,  $\delta_1 = 0.44$  and  $\delta_2 = 0.032$  as an example[17] and depict the the relationships between the two viral decay rates and treatment effects in Figure 4.

**Place of Figure 4**

The first viral decay rate,  $d_1$ , is a linear function of treatment efficacy ( $e_1$ ) in the productively infected cell compartment (Figure 4a). If the treatment is assumed perfect

in the productively infected cell compartment, i.e.,  $e_1 = 1$ , we can see, from the formula (7), that the first viral decay rate is exactly the clearance rate of productively infected cells, i.e.,  $d_1 = \delta_1$ . As mentioned above, if we assume that  $\frac{r_1}{c} \approx 1$ , then  $d_1 \approx e_1 \delta_1$ . This result was used to define a relative efficacy (RE) of two treatments (say A and B) by Essunger et al. [11], i.e., the RE of treatment A versus B is defined as  $RE = d_1^A/d_1^B = e_1^A/e_1^B$ . We can see that this definition only considered the productively infected cell compartment.

Formula (8) shows that the second decay rate,  $d_2$ , can be affected by treatment effects in both compartments,  $e_1$  and  $e_2$ . A nonlinear relationship between  $d_2$  and  $e_1$  is shown in Figure 4b. But the strong nonlinearity occurs only in the region of  $e_1 < 0.3$ , which may be unlikely for the potent cocktail anti-HIV therapies. From Figure 4c, we can see a linear relationship between  $d_2$  and  $e_2$ . We notice that, from Figure 4, if the treatment effects are strong enough, say,  $e_1 > 0.5$  and  $e_2 > 0.5$ , then the treatment has little effect on the second viral decay rate  $d_2$  (less than  $(100 \times \frac{r_2}{c})\% \leq 10\%$ ). But for weak treatments, the effect of  $e_1$  and  $e_2$  on  $d_2$  is significant. Thus the second viral decay rate  $d_2$  does provide information to distinguish between potent and weak treatments.

Based on the results from previous sections, we propose evaluating the potency (efficacy) of two antiviral treatments by comparing the viral decay rates between two randomized treatment arms. In clinical studies, randomization will ensure that the parameters  $r_1/c, r_2/c, \delta_1$  and  $\delta_2$  are homogeneous for two treatment arms. In this case, any difference found in viral decay rates between two arms is due to treatment effects. Thus, the larger the viral decay rates are, the more potent the antiviral treatment is. To compare the viral decay rates, some statistical methods need to be further explored. Some preliminary results on the statistical issues are reported in Ding and Wu [18]. Both simulation results and real clinical data analysis showed that the viral decay rates,  $d_1$  and  $d_2$ , are appropriate to be used for assessing the potency of antiviral therapies in clinical applications [18].

## 5. CONCLUSIONS AND DISCUSSIONS

We have shown that the two viral decay rates of plasma virus during the early stage of antiviral treatment are directly related to the treatment potency for inhibiting virus replication *in vivo*. We propose evaluating the antiviral efficacy of treatments using viral decay rates in the biphasic HIV dynamic model, particularly for Phase I/II clinical studies where it is very important to assess antiviral activities of a new therapy in a timely manner. We also notice that only treatment effect in productively infected cell compartment ( $e_1$ ) is related to the first phase decay rate ( $d_1$ ). However, treatment effects ( $e_1$  and  $e_2$ ) in both compartments considered in this paper are related to the second phase decay rate ( $d_2$ ). Thus, the second phase decay rate may be more important to long-term treatment success [19]. However, since current antiviral therapies are so potent as to suppress viral load below detection limit of assays very rapidly, it is very difficult to estimate the second phase decay rate unless more sensitive viral load assays are available and more frequent measurements during the second phase are taken [19].

In this paper, we considered that latently infected cell compartment was similar to that of long-lived infected cell compartment. We did not distinguish them in our models. However, if we model the activation of latent cells into productively infected cells which is similar to that in Perelson et al. [8], the results are quite similar to the models used in this paper (data not shown). In this paper, we assumed that the treatment effects were constants over the treatment time. However, this may not be true in the real world. In fact, the treatment effects may vary as the concentration of antiviral drugs varies during dose intervals. The constant treatment effects in our model can be treated as average effects. Also in practice, patients' viral load may rebound due to noncompliance and drug resistance. In this case, it will be difficult to estimate the biphasic viral decays in plasma virus. Mathematical and statistical methods need to be developed to deal with this situation. Other virologic and clinical endpoints are also important to evaluate the

long-term effect of antiviral therapies against drug resistance and noncompliance.

## ACKNOWLEDGMENT

This work was partially supported by NIAID/NIH research grants No. AI43220 and No. U01 AI38855. The authors thank Drs. Daniel Kuritzkes and Michael Lederman for discussions on clinical and virological issues, and Professor Victor DeGruttola for his comments and suggestions. The authors are also indebted to the referees for their valuable suggestions and comments.

## APPENDIX A: SOLUTION TO VIRAL DYNAMIC MODELS

Model (2) is a system of linear differential equations. Therefore the solution is clearly of the form (3), where parameters  $-c$ ,  $-d_0$ ,  $-d_1$  and  $-d_2$  ( $d_0 \geq d_1 \geq d_2$ ) are eigenvalues of the coefficients matrix of differential equation system (2):

$$A = \begin{pmatrix} -\delta_1 & 0 & (1 - \gamma_1)\alpha_1 kT & 0 \\ 0 & -\delta_2 & (1 - \gamma_2)\alpha_2 kT & 0 \\ (1 - \eta_1)(1 - \eta_0)N_1\delta_1 & (1 - \eta_2)(1 - \eta_0)N_2\delta_2 & -c & 0 \\ (\eta_0 + (1 - \eta_0)\eta_1)N_1\delta_1 & (\eta_0 + (1 - \eta_0)\eta_2)N_2\delta_2 & 0 & -c \end{pmatrix}.$$

Clearly,  $-c$  is an eigenvalue of  $A$ . Since  $-c$  is also the only nonzero element in the last column of  $A$ , the other three eigenvalues  $-\delta_0$ ,  $-\delta_1$  and  $-\delta_2$  are also eigenvalues of the submatrix

$$\tilde{A} = \begin{pmatrix} -\delta_1 & 0 & (1 - \gamma_1)\alpha_1 kT \\ 0 & -\delta_2 & (1 - \gamma_2)\alpha_2 kT \\ (1 - \eta_1)(1 - \eta_0)N_1\delta_1 & (1 - \eta_2)(1 - \eta_0)N_2\delta_2 & -c \end{pmatrix}.$$

Direct calculation shows that

$$\begin{aligned}
& |\tilde{A} - \lambda I| \\
&= -(\delta_1 + \lambda)[(\delta_2 + \lambda)(c + \lambda) - (1 - \eta_2)(1 - \eta_0)N_2\delta_2(1 - \gamma_2)\alpha_2kT] \\
&\quad + (1 - \eta_1)(1 - \eta_0)N_1\delta_1(1 - \gamma_1)\alpha_1kT(\delta_2 + \lambda) \\
&= -(\delta_1 + \lambda)[(\delta_2 + \lambda)(c + \lambda) - (1 - e_2)r_2\delta_2] \\
&\quad + (1 - e_1)r_1\delta_1(\delta_2 + \lambda) \\
&= |\bar{A} - \lambda I|,
\end{aligned}$$

where

$$\bar{A} = \begin{pmatrix} -\delta_1 & 0 & (1 - e_1)r_1 \\ 0 & -\delta_2 & (1 - e_2)r_2 \\ \delta_1 & \delta_2 & -c \end{pmatrix}, \quad (9)$$

and  $r_1 = (1 - \eta_0)N_1\alpha_1kT$ ,  $r_2 = (1 - \eta_0)N_2\alpha_2kT$  are the pretreatment viral production rates through compartments  $T_1$  and  $T_2$ . Thus,  $-d_0$ ,  $-d_1$  and  $-d_2$  are also the eigenvalues of matrix  $\bar{A}$ , which means that they are functions of  $\delta_1$ ,  $\delta_2$ ,  $c$ ,  $r_1$ ,  $r_2$ ,  $e_1$  and  $e_2$ .

## APPENDIX B: PROOF OF THEOREM 1

Here we fix  $\delta_1$ ,  $\delta_2$ ,  $c$ ,  $r_1$  and  $r_2$  and consider the effects of  $e_1$  and  $e_2$  on the viral decay rates  $d_1$  and  $d_2$ . Denote  $d_1(e_1, e_2)$  and  $d_2(e_1, e_2)$  as the viral decay rates, which are functions of  $e_1$  and  $e_2$ .

Notice that from direct calculation of eigenvalues of  $\bar{A}$  in Appendix A,

$$\begin{aligned}
d_0(1, e_2) &= \frac{(\delta_2 + c) + \sqrt{(\delta_2 - c)^2 + 4(1 - e_2)r_2\delta_2}}{2} \\
d_1(1, e_2) &= \delta_1 \\
d_2(1, e_2) &= \frac{(\delta_2 + c) - \sqrt{(\delta_2 - c)^2 + 4(1 - e_2)r_2\delta_2}}{2}.
\end{aligned} \quad (10)$$

We are going to prove Theorem 1 using this fact and the expressions of partial derivatives of  $d_0$ ,  $d_1$  and  $d_2$ .

By definition,  $d_0(e_1, e_2)$ ,  $d_1(e_1, e_2)$  and  $d_2(e_1, e_2)$  are solutions of the equation  $|\bar{A} + xI| =$

0, and

$$|\overline{A} + xI| = [x - d_0(e_1, e_2)][x - d_1(e_1, e_2)][x - d_2(e_1, e_2)].$$

On the other hand,

$$\begin{aligned} |\overline{A} + xI| &= \begin{vmatrix} x - \delta_1 & 0 & (1 - e_1)r_1 \\ 0 & x - \delta_2 & (1 - e_2)r_2 \\ \delta_1 & \delta_2 & x - c \end{vmatrix} \\ &= \begin{vmatrix} x - \delta_1 & 0 & 0 \\ 0 & x - \delta_2 & (1 - e_2)r_2 \\ \delta_1 & \delta_2 & x - c \end{vmatrix} - (1 - e_1)r_1\delta_1(x - \delta_2) \\ &= [x - d_0(1, e_2)][x - d_1(1, e_2)][x - d_2(1, e_2)] - (1 - e_1)r_1\delta_1(x - \delta_2). \end{aligned}$$

Combine the above two formulae, we have

$$\begin{aligned} &[x - d_0(e_1, e_2)][x - d_1(e_1, e_2)][x - d_2(e_1, e_2)] \\ &= [x - d_0(1, e_2)][x - d_1(1, e_2)][x - d_2(1, e_2)] - (1 - e_1)r_1\delta_1(x - \delta_2). \end{aligned} \tag{11}$$

Differentiating both sides of (11) with respect to  $e_1$  at points  $x = d_0(e_1, e_2)$ ,  $x = d_1(e_1, e_2)$ ,  $x = d_2(e_1, e_2)$ , respectively, we have

$$\begin{aligned} -\frac{\partial}{\partial e_1}d_0(e_1, e_2)[d_0(e_1, e_2) - d_1(e_1, e_2)][d_0(e_1, e_2) - d_2(e_1, e_2)] &= r_1\delta_1(d_0(e_1, e_2) - \delta_2), \\ -\frac{\partial}{\partial e_1}d_1(e_1, e_2)[d_1(e_1, e_2) - d_0(e_1, e_2)][d_1(e_1, e_2) - d_2(e_1, e_2)] &= r_1\delta_1(d_1(e_2, e_1) - \delta_2), \\ -\frac{\partial}{\partial e_1}d_2(e_1, e_2)[d_2(e_1, e_2) - d_0(e_1, e_2)][d_2(e_1, e_2) - d_1(e_1, e_2)] &= r_1\delta_1(d_2(e_1, e_2) - \delta_2). \end{aligned} \tag{12}$$

Or equivalently

$$\begin{aligned} \frac{\partial}{\partial e_1}d_0(e_1, e_2) &= -r_1\delta_1(d_0(e_1, e_2) - \delta_2)/\{[d_0(e_1, e_2) - d_1(e_1, e_2)][d_0(e_1, e_2) - d_2(e_1, e_2)]\}, \\ \frac{\partial}{\partial e_1}d_1(e_1, e_2) &= -r_1\delta_1(d_1(e_1, e_2) - \delta_2)/\{[d_1(e_1, e_2) - d_0(e_1, e_2)][d_1(e_1, e_2) - d_2(e_1, e_2)]\}, \\ \frac{\partial}{\partial e_1}d_2(e_1, e_2) &= -r_1\delta_1(d_2(e_1, e_2) - \delta_2)/\{[d_2(e_1, e_2) - d_0(e_1, e_2)][d_2(e_1, e_2) - d_1(e_1, e_2)]\}. \end{aligned} \tag{13}$$

Therefore

$$\begin{aligned}
d_0(e_1, e_2) &= d_0(1, e_2) + r_1 \delta_1 \int_{x=e_1}^1 \frac{(d_0(x, e_2) - \delta_2)}{\{[d_0(x, e_2) - d_1(x, e_2)][d_0(x, e_2) - d_2(x, e_2)]\}} dx \\
d_1(e_1, e_2) &= d_1(1, e_2) + r_1 \delta_1 \int_{x=e_1}^1 \frac{(d_1(x, e_2) - \delta_2)}{[d_1(x, e_2) - d_0(x, e_2)][d_1(x, e_2) - d_2(x, e_2)]} dx \\
d_2(e_1, e_2) &= d_2(1, e_2) + r_1 \delta_1 \int_{x=e_1}^1 \frac{(d_2(x, e_2) - \delta_2)}{[d_2(x, e_2) - d_0(x, e_2)][d_2(x, e_2) - d_1(x, e_2)]} dx
\end{aligned} \tag{14}$$

For any fixed  $0 \leq e_2 < 1$ , we have that  $d_2(1, e_2) < \delta_2 < d_1(1, e_2) = \delta_1 < c < d_0(1, e_2)$  from the result (10). Combining with the second formula in (14), this implies that  $\frac{\partial}{\partial e_1} d_1(1, e_2) > 0$ . Therefore  $d_1(e_1, e_2) < \delta_1$  in a small neighborhood of  $e_1 = 1$ . Because  $d_0$ ,  $d_1$  and  $d_2$  are continuous functions in  $e_1$  and  $e_2$ , the conclusion (a) in Theorem 1,  $d_2 < \delta_2 < d_1 < \delta_1 < c < d_0$ , is true at least in a small neighborhood of  $e_1 = 1$ .

If the conclusion (a) in Theorem 1 does not hold for all  $0 \leq e_1, e_2 < 1$ , then (14) implies that there exist values of  $(e_{10}, e_{20})$  such that  $d_1(e_{10}, e_{20}) = \delta_2 > d_2(e_{10}, e_{20})$ . (Otherwise, for each fixed  $e_2$ , as  $e_1$  decreases from 1 to 0,  $d_0$  increases,  $d_2$  decreases, and  $d_1$  decreases but never reaches  $\delta_2$ , which means that (a) holds for all  $e_1, e_2$ .) We shall show that this leads to contradictions by considering the higher order partial derivatives of the decay rates with respect to  $e_1$  at  $(e_1, e_2) = (e_{10}, e_{20})$ .

Notice that if we differentiate both sides of (11) more than twice, the right hand side will be equal to zero. The left hand side can be simplified when  $d_1(e_{10}, e_{20}) = \delta_2$ . Since  $d_1(e_{10}, e_{20}) = \delta_2 > d_2(e_{10}, e_{20})$ , (13) implies that  $\frac{\partial}{\partial e_1} d_1(e_{10}, e_{20}) = 0$ . By induction, the left side of (11) being differentiated with respect to  $e_1$  for  $k$  times equals

$$-\frac{\partial^k}{\partial e_1^k} d_1(e_1, e_2) [d_1(e_1, e_2) - d_0(e_1, e_2)] [d_1(e_1, e_2) - d_2(e_1, e_2)],$$

and hence  $\frac{\partial^k}{\partial e_1^k} d_1(e_1, e_2) = 0$ . However,  $\frac{\partial^k}{\partial e_1^k} d_1(e_1, e_2) = 0, k = 1, 2, \dots$  implies that  $d_1(e_1, e_2) = \delta_2$  for all  $e_1$ , which contradicts (10).

Now we see that (a) must hold for all  $0 \leq e_1, e_2 < 1$ .

Combine result (a) with formulas (13), we have

$$\frac{\partial}{\partial e_1} d_0(e_1, e_2) < 0 \quad \frac{\partial}{\partial e_1} d_1(e_1, e_2) > 0 \quad \frac{\partial}{\partial e_1} d_2(e_1, e_2) > 0. \tag{15}$$

Therefore the result in (b) holds for fixed  $e_2$ .

For fixed  $e_1$ , similar to (11)

$$\begin{aligned} & [x - d_0(e_1, e_2)][x - d_1(e_1, e_2)][x - d_2(e_1, e_2)] \\ = & [x - d_0(e_1, 1)][x - d_1(e_1, 1)][x - d_2(e_1, 1)] - (1 - e_2)r_2\delta_2(x - \delta_1). \end{aligned} \quad (16)$$

Differentiating both sides of (16) with respect to  $e_2$ , we yields formulas similar to (13),

$$\begin{aligned} \frac{\partial}{\partial e_2}d_0(e_1, e_2) &= -r_2\delta_2(d_0(e_1, e_2) - \delta_1)/\{[d_0(e_1, e_2) - d_1(e_1, e_2)][d_0(e_1, e_2) - d_2(e_1, e_2)]\}, \\ \frac{\partial}{\partial e_2}d_1(e_1, e_2) &= -r_2\delta_2(d_1(e_1, e_2) - \delta_1)/\{[d_1(e_1, e_2) - d_0(e_1, e_2)][d_1(e_1, e_2) - d_2(e_1, e_2)]\}, \\ \frac{\partial}{\partial e_2}d_2(e_1, e_2) &= -r_2\delta_2(d_2(e_1, e_2) - \delta_1)/\{[d_2(e_1, e_2) - d_0(e_1, e_2)][d_2(e_1, e_2) - d_1(e_1, e_2)]\}. \end{aligned} \quad (17)$$

Combine this with result (a), , we have

$$\frac{\partial}{\partial e_2}d_0(e_1, e_2) < 0 \quad \frac{\partial}{\partial e_2}d_1(e_1, e_2) < 0 \quad \frac{\partial}{\partial e_2}d_2(e_1, e_2) > 0, \quad (18)$$

which implies the result in (b) for fixed  $e_1$ .

### APPENDIX C: A FORMULA FOR APPROXIMATING $d_2$

From the third formula in (17)

$$d_2(e_1, e_2) = d_2(e_1, 1) + r_2 \delta_2 \int_{x=e_2}^1 \frac{(d_2(e_1, x) - \delta_1)}{[d_2(e_1, x) - d_0(e_1, x)][d_2(e_1, x) - d_1(e_1, x)]} dx \quad (19)$$

From direct calculation of the eigenvalues,

$$d_2(e_1, 1) = \delta_2. \quad (20)$$

Therefore we can simplify (19) as

$$d_2(e_1, e_2) = \delta_2 + r_2 \delta_2 \int_{x=e_2}^1 \frac{(d_2(e_1, x) - \delta_1)}{[d_2(e_1, x) - d_0(e_1, x)][d_2(e_1, x) - d_1(e_1, x)]} dx. \quad (21)$$

This result is used to obtain the approximation formula for  $d_2$  in Section 3.2.

## References

- [1] S. Merrill, AIDS: background and the dynamics of the decline of immunocompetence, In *Theoretical Immunology*, Part 2, A.S. Perelson, Ed., Addison-Wesley, Redwood City, Calif., 1987.
- [2] A. McLean, HIV infection from an ecological viewpoint. *Theoretical Immunology, Part Two*, A.S. Perelson, ed., 77-84 (1988).
- [3] R.M. Anderson and R.M. May, Complex dynamical behavior in the interaction between HIV and the immune system, In *Cell to Cell Signaling: From Experiments to Theoretical Models*, A. Goldbeter, Ed., New York: Academic, 1989.
- [4] A.S. Perelson, Modeling the interaction of the immune system with HIV, in *Mathematical and Statistical Approaches to AIDS Epidemiology* (Lect. Notes Biomath., Vol. 83), C. Castillo-Chavez, Ed., New York: Springer-Verlag, 1989.
- [5] D.D. Ho, A.U. Neumann, A.S. Perelson, W. Chen, J.M. Leonard, and M. Markowitz, Rapid turnover of plasma virions and CD4 lymphocytes in HIV-1 infection, *Nature*, 373, 123-126 (1995).
- [6] X. Wei, S.K. Ghosh, M.E. Taylor, V.A. Johnson, E.A. Emini, P. Deutsch, J.D. Lifson, S. Bonhoeffer, M.A. Nowak, B.H. Hahn, M.S. Saag, and G.M. Shaw, Viral dynamics in Human Immunodeficiency Virus Type 1 infection, *Nature*, 373, 117-122 (1995).
- [7] A.S. Perelson, A.U. Neumann, M. Markowitz, J.M. Leonard, D.D. Ho, HIV-1 dynamics in vivo: Virion clearance rate, infected cell life-span, and viral generation time, *Science*, 271, 1582-1586 (1996).
- [8] A.S. Perelson, P. Essunger, Y. Cao, M. Vesanen, A. Hurley, K. Saksela, M. Markowitz, and D.D. Ho, Decay characteristics of HIV-1-infected compartments during combination therapy, *Nature*, 387, 188-191 (1997).

- [9] D.W. Notermans, J. Goudsmit, S.A. Danner, F. de Wolf, A.S. Perelson and J. Mittler, Rate of HIV-1 decline following antiretroviral therapy is related to viral load at baseline and drug regimen, *AIDS*, 12, 1483-1490 (1998).
- [10] H. Wu, D.R. Kuritzkes, M.S. Clair, H. Kessler, E. Connick, A. Landay, M. Heath-Chiozzi, F. Rousseau, L. Fox, J. Spritzler, J.M. Leonard, D.R. McCleron, and M.M. Lederman, Interpatient variation of viral dynamics in HIV-1 infection: Modeling results of AIDS Clinical Trials Group Protocol 315, The International Workshop on HIV Drug Resistance, Treatment Strategies and Eradication, Abstract 99, 66-67 (1997).
- [11] P. Essunger, M. Markowitz, D.D. Ho, and A. S. Perelson, Efficacy of drug combination and dosing regimen in antiviral therapy, The International Workshop on HIV Drug Resistance, Treatment Strategies and Eradication, Abstract 73, 48 (1997).
- [12] D.D. Ho, Novel approaches for the evaluation of new drugs: Approaches using viral dynamics. The 5th Conference on Retroviruses and Opportunistic Infections. Chicago, IL, February 1998;
- [13] R.M.W. Hoetelmans, M.H.E. Reijers, G.F. Weberling, S. Furriaans, and F.M.A. Lange, The rate of decline of HIV-1 RNA in plasma correlates with nelfinavir concentrations in plasma. The 12th World AIDS Conference. Geneva, Switzerland, June 28-July 3, 1998.
- [14] M. Piatak, M.S. Saag, L.C. Yang, S.J. Clark, J.C. Kappes, K.-C. Luk, B.H. Hahn, G.M. Shaw, and J.D. Lifson, High levels of HIV-1 in plasma during all stages of infection determined by competitive PCR, *Science*, 259, 1749-54 (1993).
- [15] H. Wu, and A.A. Ding, Population HIV-1 dynamics in vivo: applicable models and inferential tools for virological data from AIDS clinical trials, to appear in *Biometrics* Vol. 55, No. 2 (1999).

- [16] A.V.M. Herz, S. Bonhoeffer, R.M. Anderson, R.M. May, and M.A. Nowak, Viral dynamics in vivo: Limitations on estimates of intracellular delay and virus decay, *Proc. Natl. Acad. Sci. USA*, 93, 7247-7251 (1996).
- [17] H. Wu, D.R. Kuritzkes, D.R. McCleron, H. Kessler, E. Connick, A. Landay, M. Heath-Chiozzi, F. Rousseau, L. Fox, J. Spritzler, J.M. Leonard, D.R. McCleron, and M.M. Lederman, Characterizing viral dynamics in HIV-1-infected patients treated with combination antiretroviral therapy: relationships to host factors, cellular restoration and virological endpoints, *Journal of Infectious Diseases*, in press (1999).
- [18] A.A. Ding and H. Wu, Assessing antiviral potency of anti-HIV therapies in vivo by comparing viral decay rates in viral dynamic models, submitted to *Journal of the Royal Statistical Society, Series A*.
- [19] H. Wu, How frequently should viral load be monitored to evaluate antiretroviral therapies in AIDS clinical trials? *Journal of Acquired Immune Deficiency Syndromes and Human Retrovirology*, in press (1999).

Table 1: Parameter Values Used in the Simulation Studies

Parameters	Values	Parameters	Values
$\gamma_1$	0.5, 0.1	$\eta_0$	0.99
$\gamma_2$	0.3, 0.1	$\eta_1$	0.8
$\alpha_1$	0.9	$\eta_2$	0.6
$\alpha_2$	0.1	$e_1$	0.9, 0.19
$\delta_1$	0.44	$e_2$	0.72, 0.19
$\delta_2$	0.032	$T_1(0)$	3068
$k$	0.00015	$T_2(0)$	4688
$T$	10000	$V_I(0)$	1000
$N_1 = N_2$	200	$V_{NI}(0)$	99000
$c$	3.0		

## Figure Legends

Figure 1. Process of HIV Replication and Intervention of Antiviral Drugs. Step 1, HIV enters a target cell; Step 2, HIV uses an enzyme known as reverse transcriptase to convert its RNA into DNA (RTI drugs work at this step); Step 3, HIV DNA enters the nucleus of the target cell and inserts itself into the cell's DNA. HIV DNA then instructs the cell to make many copies of the original virus; Step 4, New virus are assembled (PI drugs work at this step) and leave the cell, ready to infect other target cells. This completes a cycle of virus replication.

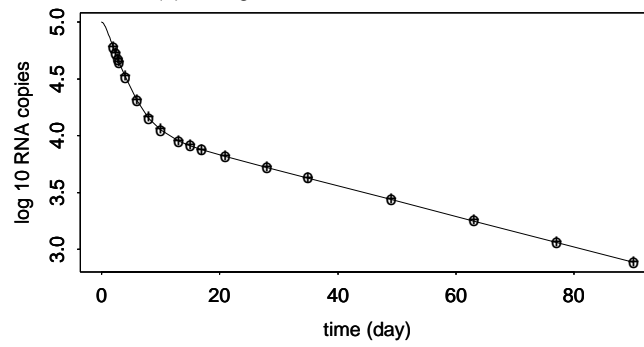
Figure 2. Simulation results on approximation formulas. Solid line is numerical solution to differential equations (2); the cross (+) is the approximation by bi-exponential model (4); the circle ( $\circ$ ) is the approximation of formulas (7) and (8).

Figure 3. Comparison between true viral decay rates (solid line) versus the estimates from our approximation formulas (dot line).

Figure 4. Relationships between viral decay rates and treatment effects.

Figure 1: Ding and Wu

(a) Strong treatment effects:  $e_1=0.9$ ,  $e_2=0.72$



(b) Weak treatment effects:  $e_1=0.19$ ,  $e_2=0.19$

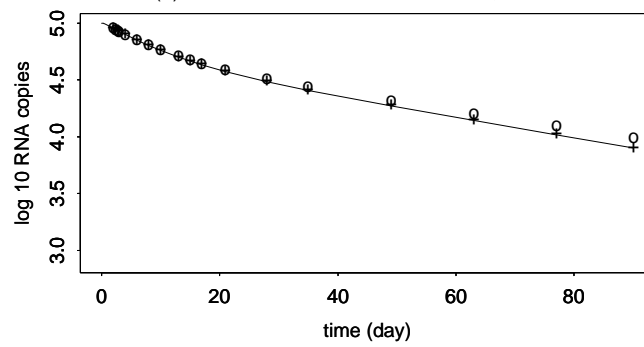


Figure 2: Ding and Wu

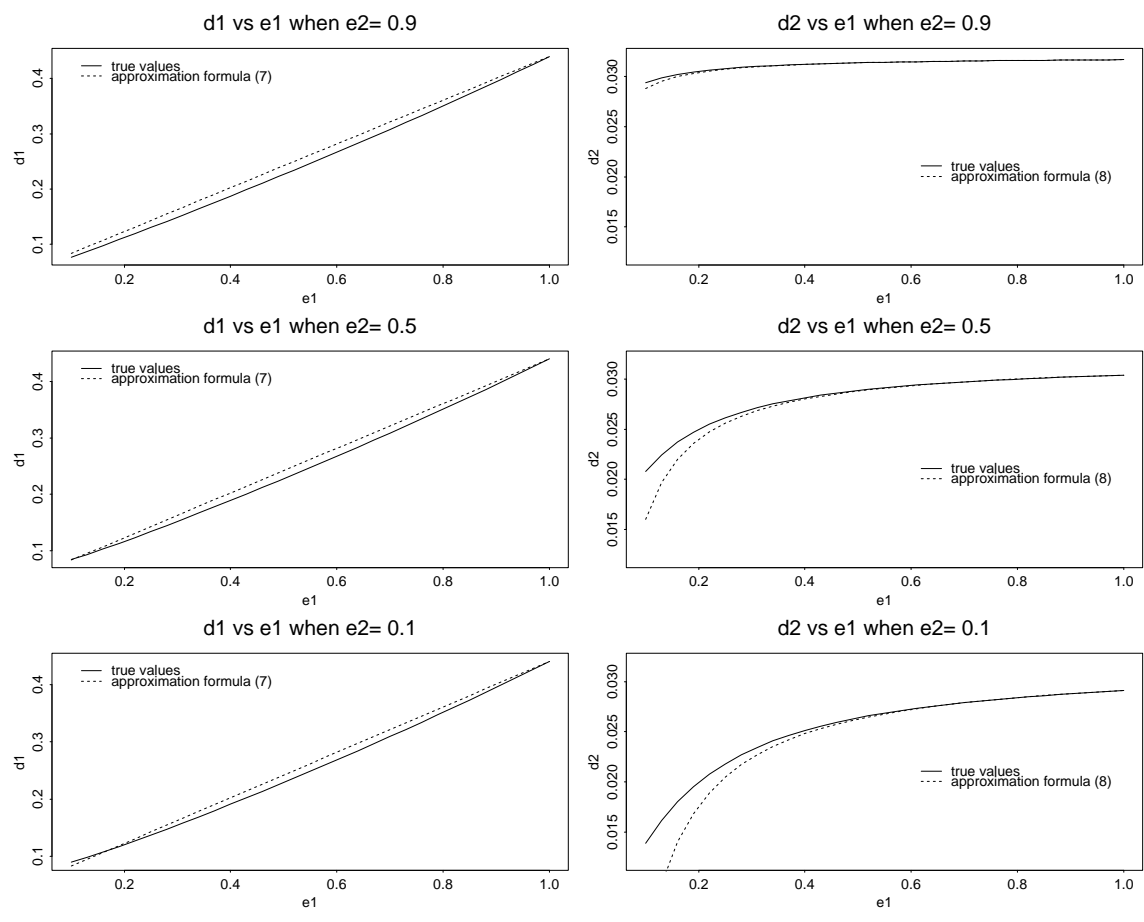


Figure 3: Ding and Wu